

Design and Construction of an Industrial Blender

Jose Manuel Ramirez Quintero¹, Luz Karime Hernández Gegén² and Sir-Alexci Suarez Castrillon³

^{1,2} Faculty of Engineering and Architecture. University of Pamplona, Colombia.

³ Engineering Faculty, University Francisco of Paula Santander Ocaña, Colombia.

Abstract

This work shows the design and construction of an industrial blender, taking as a basis the different types of industrial blenders that exist in the market, with the objective of optimizing times, increasing the yield and the production of ice cream. For analysis purposes, a viscosity test of the commercial ice cream mixture is carried out, in order to determine what type of fluid it is and to find the shear stress of the mixture, in this way the type of blades and shaft of the blender is determined. On the other hand, the structure that will support the blender is analyzed and other parts are selected depending on the need.

Keywords: Design, stress, viscosity, industrial blender.

1. INTRODUCTION

In ice cream production, there are different manufacturing scenarios, i.e., multi-plant (MP), single plant (SP), distributed manufacturing (DM), food incubator (FI) and home manufacturing (HM), which cover a wide range of scales (0.01 kg/h to 50,000 kg/h) and increase decentralized production [1]. Large-scale industries usually have automated processes, which facilitates product processing, increases the production volume, as well as the safety and hygiene of their operators. The production processes in companies with similar capacity are practically the same, but differ in aspects such as the raw materials and machines used. In contrast, regional companies, unlike large ice cream producers, do not have the same technification in their production process due to the high percentage of manual activities during the process, making the result more artisanal.

Studies converge on the importance of the mixing or agitation process as an essential and prevalent operation in the processing of dairy products in order to promote uniformity, dissolution and heat transfer when making ice cream [2]. If this process is not carried out correctly, there will not be a uniform mixing of the ingredients, which will cause the amounts of nutrients present in the final product to be inadequate. Associated to this, product safety will be low and this will affect the quality of the product, according to Rodriguez [3]. Regarding the raw material and the machine, authors Calle and Quispe agree that the flow that guarantees uniform distribution of the components is generally obtained with mechanical procedures, such as agitation carried out continuously in tanks [4], [5]. For this purpose, the efficiency of the machine is important, because the more movement it exerts on the particles of the ingredients, the better the quality of the product [3]. Mixing of liquids and solids, fragmentation of solids and liquids, multiphase behavior and interactions with complex

machine geometries are substantial challenges for food processing operations [6].

According to Bohórquez the type of product, the amount of raw material to be processed and the agitation speed should be considered when choosing the mixing equipment where the mixture is produced. The inadequate selection of these aspects will not only affect the quality of the product, but also the operation of the mixing equipment [7]. To complete the scheme of parameters to be considered, the shape of the vessel should be mentioned, since according to Caiza, a good mixing element can be useless in an inappropriate vessel [8].

This research article presents the development of the design and construction of a blending system for ice cream. It is proposed a design that allows to have continuity in the process and to obviate some manual procedures in small and medium companies. Finally, it is expected to optimize production times, the operation process and its safety.

2. METHOD

For the design of the blender, the anthropometric measurements of the Colombian woman will be taken into account, see Figure 1, since in the company under study, the production area is only handled by women. For this reason, the hopper filling process performed by the operators manually, limits the size of the blender to be designed.

Considering Table 1, the average height of the Colombian woman between 20 and 39 years old is 156.9 cm, therefore, the adequate height for the blender will be 1 m.

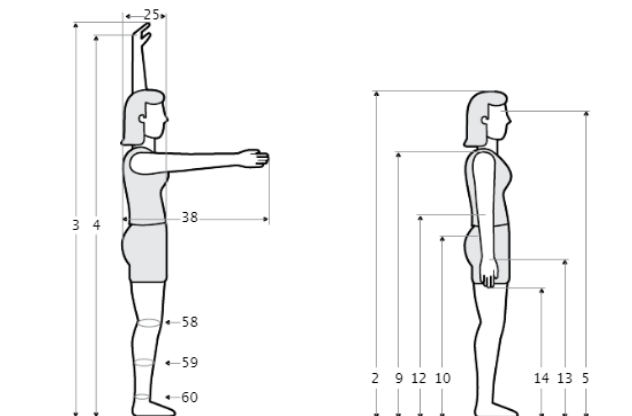


Fig. 1. Anthropometric measurements of a Colombian woman between 20 and 39 years of age. **Source:** [9]

Table 1. Average dimensions of a Colombian woman between 20 and 39 years of age.

Dimensiones	20 - 29 años (n= 233)					30 - 39 años (n= 256)				
	\bar{x}	D.E.	Percentiles			\bar{x}	D.E.	Percentiles		
			5	50	95			5	50	95
1 Masa corporal (Kg)	56.6	8.85	45.2	55.3	71.4	59.3	8.57	46.9	58.9	74.5
2 Estatura (cm)	156.9	5.80	148.0	156.3	166.4	155.8	5.43	148.3	155.6	166.1
3 Alcance vertical máximo	196.2	8.08	184.5	195.7	209.4	195.1	7.67	184.1	194.9	209.5
4 Alcance vertical con asiento	182.3	7.61	171.0	181.6	194.8	181.7	7.38	170.6	181.9	195.1
5 Altura de los ojos	146.3	5.65	137.5	146.1	155.4	145.4	5.23	137.9	145.0	154.9
9 Altura acromial	128.0	5.05	120.3	127.8	136.3	127.3	4.85	120.3	126.8	135.8
10 Altura cresta ilíaca medial	93.4	4.25	86.7	93.5	100.5	92.6	4.24	86.6	92.2	100.5
12 Altura radial	98.9	4.04	92.7	98.8	105.6	98.3	3.86	92.3	97.9	105.0
13 Altura estilóidea	75.8	3.30	70.5	75.5	81.3	75.3	3.19	70.4	75.1	80.6
14 Altura dactílea dedo medio	59.9	2.88	55.1	59.8	64.8	59.5	2.75	55.0	59.2	64.0
25 Anchura del tórax	17.6	1.65	15.2	17.5	20.8	18.4	1.75	15.5	18.5	21.5
38 Alcance anterior brazo	65.4	3.11	61.0	65.2	70.7	65.7	3.12	60.9	65.6	71.3
58 Perímetro rodilla media	34.8	2.60	31.3	34.8	39.4	35.4	2.58	31.4	35.2	40.3
59 Perímetro pierna media	33.7	2.57	30.0	33.6	38.1	34.1	2.39	30.5	34.0	38.6
60 Perímetro supramoleolar	20.5	1.45	18.3	20.4	23.0	20.5	1.27	18.5	20.6	22.8

Source: [9]

Figure 2 shows the preliminary design of the blender.

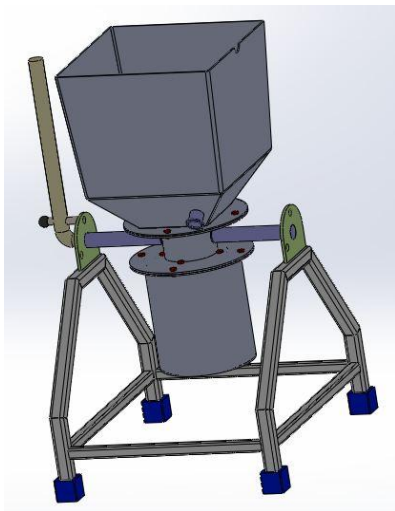


Fig. 2. Blender of the proposed liquefying system

2.1 Supporting structure design and structural analysis

Taking into account the design criteria, specifically the dimensions, square profiles of 40x40x4mm and 30x30x2.6mm were used for the construction of the structure that will support the weight of the assembly. See **Fig. 3**.

Height of the structure: 52cm

Base: 74cmx64cm

Quantity of profiles 40x40x4: 10

Number of profiles 30x30x2.6: 4

Structural analysis

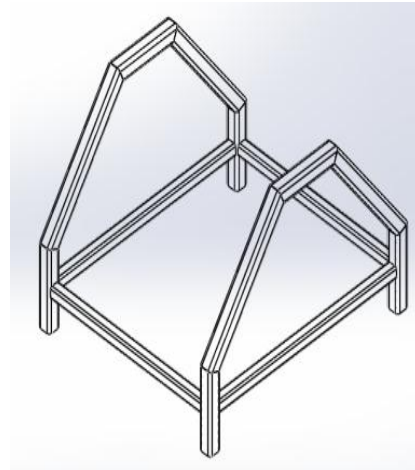


Fig. 3 . Structure of the proposed liquefaction system

The structural analysis was made based on the element shown in Figures 4 and 5, which was considered as a beam. Since the structure is symmetrical, only half of it was analyzed. This analysis is carried out in order to calculate the maximum moment supported by the element and thus establish the maximum stress to which the structure will be subjected.

The following parameters were taken into account for the analysis, as detailed below:

Motor weight 2Hp: 33kgf

Weight of the product to be mixed per liter: 1Kgf/L

Safety factor: 2

Volume of the vessel: 75L

Weight/liter: 150Kgf/75L

Average weight of accessories: 10Kgf

Total load to be supported: 193Kgf

193kg=1893.33N

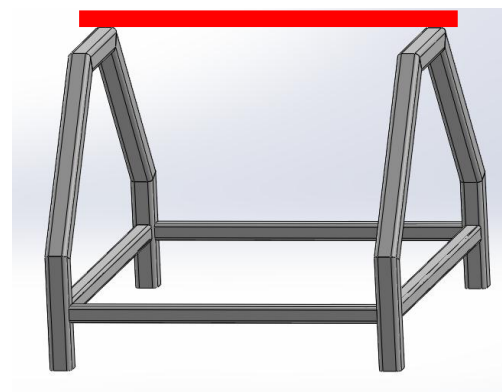


Fig. 4. Structural analysis

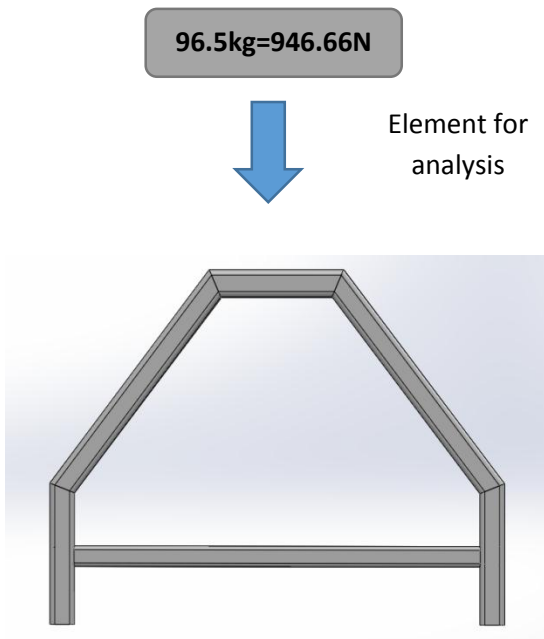


Fig. 5. Structural analysis

Free body diagram

The diagram shown in Fig. 6 shows the loads and spacings that make up the structure.

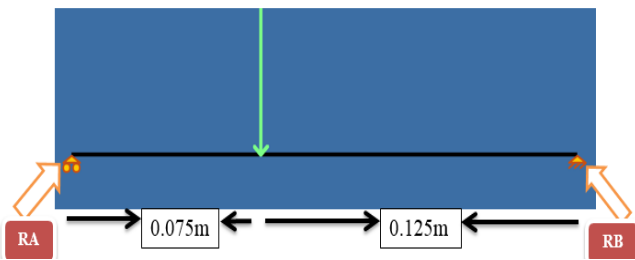


Fig. 6 . Free body diagram of the structure. Source: [10]

RA: 796.177N; RB: 477.68N; RAy: 591.675N; RBy: 354.99N
 Maximum torque: 44.375Nm

Calculation of the moment of inertia and the distance from the centroid of the element to the periphery "C".

$$e = 4\text{mm}$$

$$a = 40\text{mm}$$

$$I = \frac{bh^3}{12} = I_{\text{ext.}} - I_{\text{in}} \quad (1)$$

$$I = 1.2592 \times 10^{-7} \text{m}^4 \quad C = 0.02 \text{m}$$

$$\sigma_{\text{max}} = \frac{44.375 \text{Nm} \times 0.02 \text{m}}{1.2592 \times 10^{-7} \text{m}^4} = 7.048 \text{MPa}$$

According to this result, AISI 304 stainless steel square sections will be used with a yield stress equal to 310MPa.

$$FS = \frac{310 \text{MPa}}{7.048 \text{MPa}} = 43,98$$

This safety factor value obtained indicates that the profile made of AISI 304 steel withstands 43.98 times the applied load.

Column analysis

Element AB is analyzed as a column embedded at either ends to determine whether buckling will occur or not (see Fig. 7). To know if element AB will suffer buckling, the critical force (Fr) at which buckling will occur is calculated and compared with the force (F) to which it is subjected according to this condition:

$$F > Fr \quad \longrightarrow \quad \text{There is}$$

Where Fr is obtained by applying Euler's equation:

$$Fr = \frac{\pi^2 EI}{Le^2} \quad (2)$$

$$Le = L = 0.4036 \text{m}$$

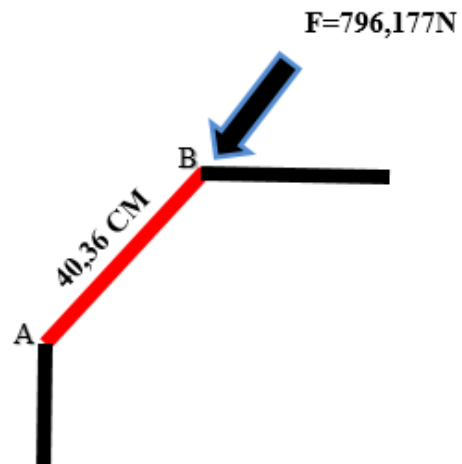


Fig. 7 . Free body diagram, member AB

$$Fr = \frac{\pi^2 (200 \times 10^9) (1.2592 \times 10^{-7})}{(0.4036)^2}$$

$$Fr = 1525 \text{KN}$$

$$F < Fr \quad 796.17 \text{KN} < 1525 \text{KN} \quad \text{No buckling}$$

2.2 Ice cream mixing rheology

Rheology, defined as the study of change in shape and flow of matter, is related to elasticity, viscosity and plasticity. Viscosity, on the other hand, is defined as the internal friction of a fluid caused by molecular attraction that makes it resistant to the tendency to flow. The Brookfield viscometer measures that friction and thus functions as a tool of rheology. The purpose of this practice was to determine the viscosity of the sample of ice cream produced in a particular ice cream company, and to find the shear stress that the fluid presents and with this, to establish the forces to which the blades will be subjected and calculate the diameter of the shaft to be used.

Brookfield viscometers, such as the one shown in **Fig. 8**, are frequently used to perform viscosity measurements of a variety of materials with Newtonian and non-Newtonian behavior. Due to the importance of such measurements in many fields of industry, there is a need to include Brookfield viscometer measurements in quality assurance systems.



Fig. 8 . BROOKFIELD DV-E viscometer. **Source:** Master's Degree in Food Engineering Laboratory, University of Pamplona.

Materials and methods

The ice cream mix sample comes from a commercial ice cream shop. The materials used for this practice are the following: Brookfield medium density viscometer, 1 beaker of 600 ml, and sample of the ice cream mixture (500 ml). See **Fig. 9**.

For this practice, a 600ml beaker was taken to which a quantity of 500ml of ice cream mixture was added. The viscosity of this sample was determined by means of the Brookfield RVDV-E medium density viscometer with spindle # 2, the viscosity data and torque percentage were displayed on the monitor of the equipment. The viscosity values were measured at all the rpm at which the equipment works as shown in **Table 2**.

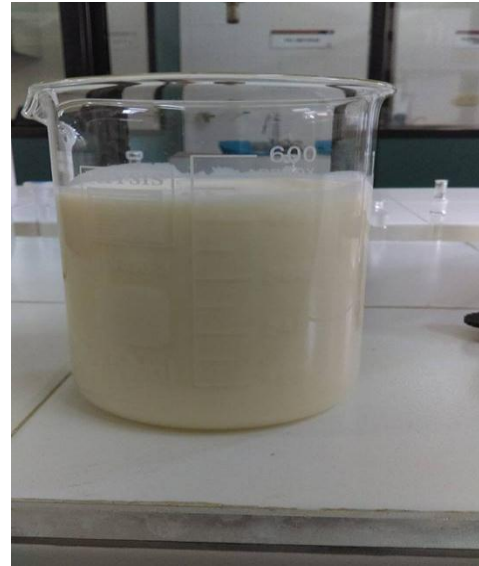


Fig. 9. Sample ice cream mix (500ml). **Source:** Master's degree in food engineering laboratory, Pamplona University.

Table 2. Viscosity analysis

VISCOSITY ANALYSIS 1		
RPM	% TORQUE	VISCOSITY (cp)
1	4.3	43000
1.5	5.1	34000
2	5.8	29000
2,5	6.6	26400
3	7.3	24300
4	8	20000
5	8.8	17600
6	9.5	15800
10	12.1	12100
12	13.2	11000
20	17.1	8550
30	20.9	6970
50	27.8	5560
60	30.4	5070
100	42.2	4220

Calculation of the torque exerted by the viscometer to move the mixture at a constant speed (in rpm)

The following equation is used to determine the percentage of torque required by the machine to move the mixture:

Torque supplied by the viscometer: 7187 dynes*cm

$$TORQUE = \frac{(7187 \text{ dynas} * cm) * \%torque}{100}$$

Calculation of angular velocity.

The angular velocity and torque are required to know the shear stress. The corresponding calculations are then performed.

$$\omega \left(\frac{du}{dr} \right) = \frac{2 * \pi * rpm}{60} = rad/s \quad (3)$$

Calculation of shear stress

Table 3 shows the dimension of the selected spindle being #2RV given its diameter. Each of the dimensions in question are shown in Figure 10

Table 3. Spindle dimensions

Spindle	Figure	C-Diameter	D	E	F
#62 LV	1	0.7370 (18.72)	0.270 (6.86)	1.000 (25.40)	1.969 (50.00)
#63 LV	1	0.4970 (12.60)	0.070 (1.78)	1.007 (25.60)	1.969 (50.00)
#1 RV	2	2.2150 (56.26)	0.885 (22.48)	1.062 (26.97)	2.406 (61.12)
#1 H	2	2.2150 (56.26)	0.908 (23.06)	1.062 (26.97)	2.406 (61.12)
#2 RV	3	1.8477 (46.93)	0.063 (1.65)	1.062 (26.97)	1.938 (49.21)
#2 H	3	1.8550 (47.12)	0.063 (1.65)	1.062 (26.97)	1.938 (49.21)
#3 RV/H	3	1.3658 (34.69)	0.063 (1.65)	1.062 (26.97)	1.938 (49.21)
#4 RV/H	3	1.0748 (27.3)	0.063 (1.65)	1.062 (26.97)	1.938 (49.21)
#5 RV/H	3	0.8324 (21.14)	0.063 (1.65)	1.062 (26.97)	1.938 (49.21)
#6 RV/H	1	0.5757 (14.62)	0.063 (1.57)	1.188 (30.17)	1.938 (49.21)

Dimensions are in inches (mm). Dimension A is 4.531 (115) on LV spindles; 5.250 (133) on RV/H spindles. Dimension B is 0.125 (3.2) on all spindles.

Source: [11]

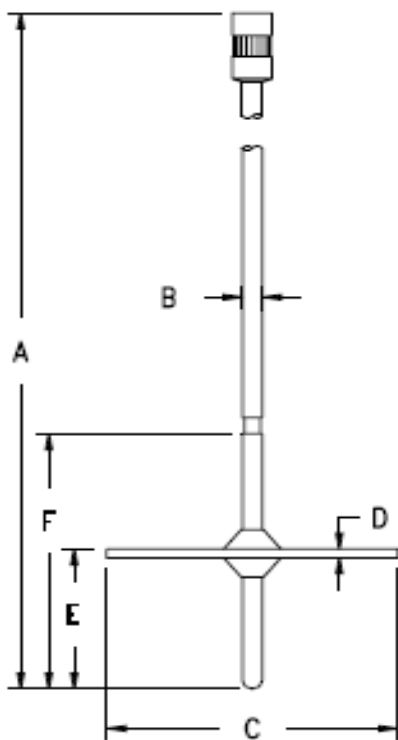


Figure 10 . Diagram of the spindle. Source: [11]

Rh= Spindle radius

Rc= Radius of container

t= Disc thickness

According to the RV-media viscometer manual the dimensions of spindle #2 are:

Rh= 2.3465 cm

Rc= 4.2 cm

t= 0.165cm

The shear stress is determined with:

$$\tau = \frac{F}{A_{\text{superficial del disco}}} \quad (4)$$

$$Torque = F * Rh \quad (5)$$

$$F = \frac{Torque}{Rh} \quad (6)$$

$$Esfuerzo\ cortante\ (\tau) = \frac{Torque}{2 * \pi * Rh^2 * t} \quad (7)$$

Table 4 shows the stress behavior as a function of speed (omega) and torque.

Table 4. Shear stress

Omega (rad/s)	Torque (dynas*cm)	Shear stress (dynas/cm ²)
0.104719755	309.041	54.12276708
0.157079633	366.537	64.19211909
0.20943951	416.846	73.0028021
0.261799388	474.342	83.07215412
0.314159265	524.651	91.88283713
0.41887902	574.96	100.6935201
0.523598776	632.456	110.7628722
0.628318531	682.765	119.5735552
1.047197551	869.627	152.2989492
1.256637061	948.684	166.1443082
2.094395102	1228.977	215.2323993
3.141592654	1502.083	263.0618214
5.235987756	1997.986	349.9099825
6.283185307	2184.848	382.6353765
10.47197551	3032.914	531.1583187

According to these results, the **du/dr (omega)** vs. **shear stress** is plotted in order to determine the equation that best fits the graph and thus find the maximum stress to which the blades will be subjected at 3600 rpm, thus determining the minimum diameter of the shaft that will be used to move the mixture.

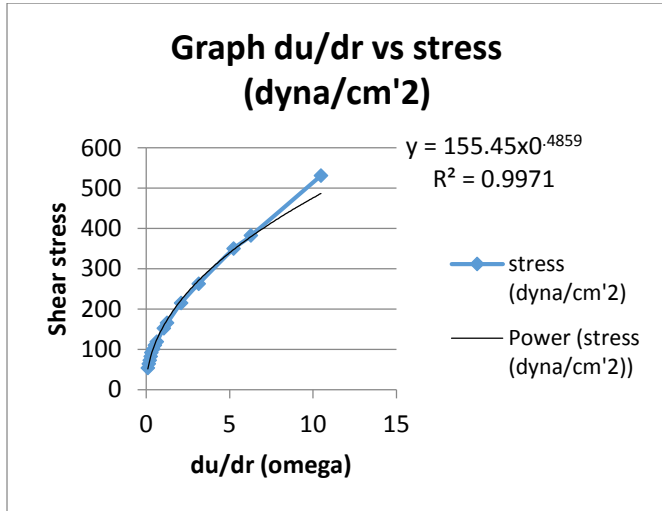


Figure 11. Angular velocity VS stress

The equation that most closely approximates the graph has a reliability of 0.9971 and is polynomial.

$$y = 155.45x0.4859$$

Where **y** is the stress and **x** the du/dr.

The tabulation of the shear stress according to the rpm applied and the graph of du/dr vs. stress already adjusted by the equation obtained is shown below. See **Table 5** and **Fig. 12**.

Table 5. Shear stress behavior

rpm	du/dr (rad/s)	Shear stress (dynes/cm ²)
1	0.104719755	51.93051527
1.5	0.157079633	63.23905545
2	0.20943951	72.72657022
2.5	0.261799388	81.05534937
3	0.314159265	88.56371986
4	0.41887902	101.8505976
5	0.523598776	113.5147134
6	0.628318531	124.0298803
10	1.047197551	158.9727298
12	1.256637061	173.6987925
20	2.094395102	222.6348292

30	3.141592654	271.1164377
50	5.235987756	347.497878
60	6.283185307	379.6875217
100	10.47197551	486.6566159
200	20.94395102	681.542757
500	52.35987756	1063.780823
1000	104.7197551	1489.781688
1500	157.0796327	1814.200886
2000	209.4395102	2086.378539
2500	261.7993878	2325.314405
3000	314.1592654	2540.714403
3600	376.9911184	2776.067469

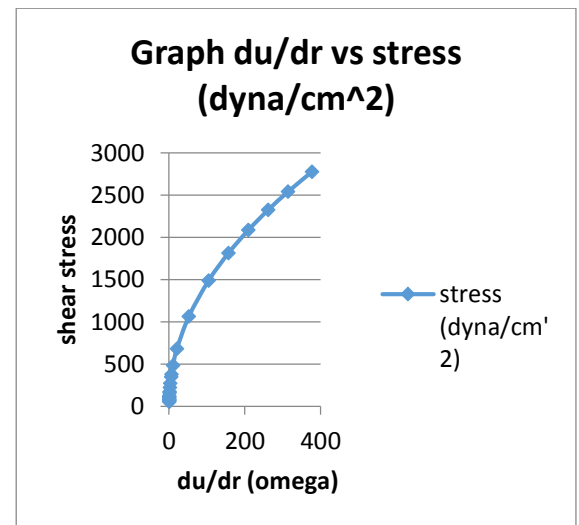


Fig. 12 . Angular velocity VS stress

The shear stress to which the liquefaction blades will be subjected is **2776.067 dynes/cm²**.

Similarly, **Fig. 13a** representation of flow curves for different fluids used to rheological characterize the ice cream mixture.

By comparing the graph obtained with this flow curve representation it can be deduced that the mixture to prepare the ice cream is a non-Newtonian thinning fluid and the equation found resembles the power law model that describes these fluids, expressed by the following equation, where **k** and **n** are constants and **n**<1.

$$\tau = k \frac{du^n}{dr} \quad (8)$$

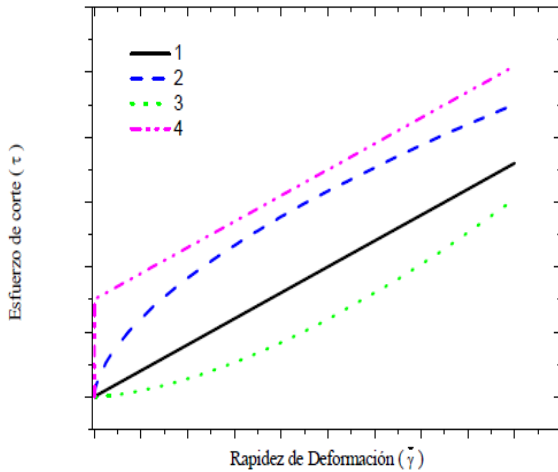


Fig. 13. Representation of flow curves for different fluids. 1) Newtonian fluid, 2) Thinning non-Newtonian fluid, 3) Dilatant non-Newtonian fluid, 4) Bingham fluid. **Source:** [12]

2.3 Shaft design

The torsional shaft design is developed based on Robert Mott's theory.

Static analysis

$T_{nominal}: 37lb \cdot in; S_y: 45000 \text{ psi}$

To calculate the minimum shaft diameter to support the motor torque, we substitute in τ_{max} for a design stress denoted by τ_d .

$$\tau_{max} = \tau_d = \frac{S_{ys}}{N} = \frac{S_y}{2N} \tag{9}$$

Where N is the design factor chosen based on the type of load to which the shaft will be subjected and S_{ys} is the shear stress of the material, in case this is not known the value can be estimated as $S_y/2$.

Table 6 will be used to determine the N value.

Table 6 . Design factors and design shear stresses for ductile metals.

Type of load	Design factor	Design shear stress $T_d = s_y/2N$
Constant static torque	2	$T_d = s_y/4$
Repeated torsion	4	$T_d = s_y/8$
Torsional impact or shock	6	$T_d = s_y/12$

Source: [13]

Taking $N=2$ we have:

$$\tau_d = \frac{45000 \text{ psi}}{4} = 11250 \text{ psi}$$

The polar section modulus denoted by Z_p will now be included.

$$Z_p = \frac{J}{c} = \frac{\pi * D^3}{16} \quad Z_p = \frac{J}{c} = \frac{\pi * D^3}{16} \tag{10}$$

para una sección sólida

$$J = \frac{\pi * D^4}{32}, \quad C = \frac{D}{2} \tag{11}$$

For a hollow section (12)

$$Z_p = \frac{\pi}{16} * \frac{D_e^4 - D_i^4}{D_e}$$

To find the value of Z_p , it will be related to the design shear stress and to the motor torque, according to the following relationship.

$$\tau_d = \frac{T_{nominal}}{Z_p} \tag{13}$$

despejando para Z_p tenemos que

$$Z_p = \frac{37lb \cdot in}{11250 \text{ lb}/in^2} = 3.288e^{-3} \text{ in}^3$$

The minimum shaft diameter would be:

$$D_{min} = \sqrt[3]{\frac{16 * Z_p}{\pi}} = 0.25 \text{ in} = 6.35 \text{ mm}$$

Blade design

For analysis purposes, the blade of the blender is considered to be completely rectangular, as shown in Fig. 14

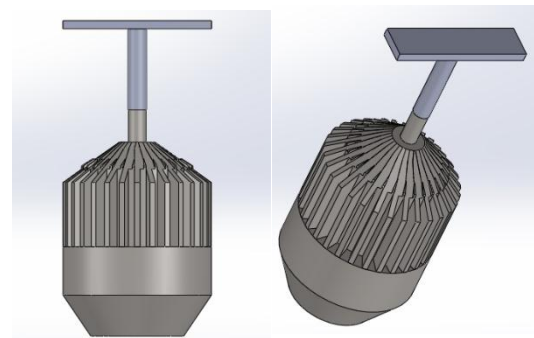


Fig. 14 . Rectangular shaped blade

$T_{nominal}: 37lb \cdot in$

Blade diameter: $16 \text{ cm} = 6.3 \text{ in}$

Loads applied to the blades

Fig. 15 shows the loads to which the blades will be subjected in order to proceed with the design of the blades.

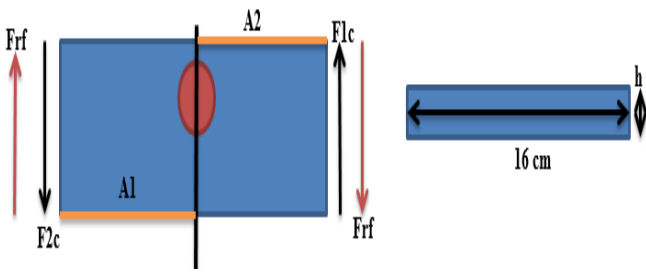


Fig. 15 . Free body diagram of the blade

Taking into account the viscosity of the mixture and the fact that the motor rotates at 3600 rpm, the shear stress generated by the fluid on the blades is equal to:

$$\tau_{\text{fluido}} = 0.04026 \text{ lb/in}^2$$

This value indicates that, for each square inch, the fluid generates a force opposite to the movement of the blades of 0.04026 lb.

Calculation of blade thickness (h)

Frf: frictional force of the ice cream mix

Fc: force exerted by the blades

As: surface area of the blade in contact with the ice cream mixture

$$\text{torque} = F * d \quad F = F1c = F2c$$

$$As = A1s = A2s$$

If the motor torque is 37lb*in and the diameter of the blades is 3.15in, the force at the end of the blades is 11.74lb.

The force exerted by the blades at their ends is 11.74 lb, to ensure that the motor can liquefy the mixture, the force exerted by the fluid on the surface area of the blade must be less than the force exerted by the motor, otherwise the motor will not be able to liquefy.

The force exerted by the fluid on the blades is now calculated:

$$\tau_{\text{fluido}} = \frac{\text{fuerza fluido (Frf)}}{As} \quad (14)$$

$$\text{donde } As = b * ht \quad \text{donde la } b = 3.15 \text{ in}$$

$$0.04026 \frac{\text{lb}}{\text{in}^2} = \frac{Frf}{(3.15\text{in}) * h1} \quad \text{despejando } h1$$

$$h1 = \frac{Frf}{0.127 \frac{\text{lb}}{\text{in}}}$$

Yes $Frf \geq F$ NO HAY LICUADO

If $Frf = F = 11.74 \text{ Lb}$

Then,

$$h1 = \frac{11.74\text{lb}}{0.127 \frac{\text{lb}}{\text{in}}} = 92.44\text{in}$$

$$ht = \frac{h1}{2} = 46.22\text{in}$$

This result means that in order for the motor to pull that mixture the blade thickness must be less than 46.22 in.

Yes $h1 = 4\text{mm} = 0.157\text{in}$

Then,

$$Frf = 0.02\text{lb y}$$

$$\tau_{fc} = \frac{2 * 0.02\text{lb}}{6.3\text{in} * 0.157\text{in}} = 0.04\text{psi}$$

τ_{fc} = Esfuerzo cortante que genera el fluido en la cuchilla

According to this result, the material in which the blade will be manufactured is a 10 gauge sheet of AISI 304 stainless steel with yield shear stress =22500 psi.

The shear stress to which the blades will be subjected is << the yield shear stress of the material, which guarantees that the blades will not fail.

Fig. 16 and Fig. 17 show the 2 blades to be used in the blender with an angle of 45° up and down.



Fig. 16 . Blender blades



Fig. 17. Fabricated blade

Coupling, bearing and mechanical seal selection

A spider coupling was used. This consists of two apples of curved "jaws" that fit together with a polyurethane "star" in between. This geometry allows it to accept good angular misalignment and also to transmit more torque smoothly. For this reason, it is widely used in pumps, speed reduction gearboxes, compressors, fans, mixers, conveyor assemblies. See Fig. 18.



Fig. 18 . Spider coupling. Source: ([14])

Benefits

- Easy assembly and axial connection.
- Good vibration absorption capacity.
- Maintenance-free (no lubrication required).
- Fail-safe (they continue to work even if the elastomer is damaged).
- They work at high speeds.

Selection procedure

For the assembly of the machine, a commercial electric motor of 2hp, 3600 rpm and a nominal torque of 37lb*in was selected.

1) Selection of the Fs. (Service Factor)

Table 7 . Service factor selection

TIPO DE TRABAJO O MÁQUINA	Motor Eléctrico		Motores de combustión			
	Torque estándar	Alto Torque	4 o más cilindros	3 cilindros	2 cilindros	1 cilindro
Operación uniforme Ejemplo: Bombas hidráulicas y centrifugas, generadores livianos, ventiladores, soplaadores, transportadores de banda o tornillo.	1.0	1.25	1.5	1.7	2.0	2.7
Operación uniforme con fluctuación moderada Máquinas para el trabajo de la madera, molinos, maquinaria textil, mezcladores.	1.6	1.8	2.0	2.3	2.5	3.0
Operación fluctuante Hornos rotativos, máquinas litográficas y de impresión, generadores, bombas para líquidos viscosos.	1.8	1.9	2.2	2.5	2.7	3.1
Operación fluctuante con choques Mezcladoras de concreto, martinets, molinos para papel, bombas de compresión, bombas de propela, entorchadoras de cable, centrifugas.	1.8	2.0	2.5	2.7	3.0	3.4
Operación muy fluctuante con choques Excavadoras, molinos de bolas, bombas de pistón, prensas de forja y estampado.	2.1	2.3	2.7	3.0	3.4	3.8
Trabajo pesado, muy fluctuante con choques fuertes Compresores y bombas de pistón, movimiento de rodillos pesados, estrusoras de ladrillo, prensas de mandibula para moler piedra.	2.5	3.1	3.3	3.6	4.0	4.5

Source: [14]

According to Table 7, a service factor of 1.6 will be used.

2) Design torque calculation

$$Td = Tnominal * Fs = 59.2 \text{ lb*in}$$

3) Coupling selection

Table 8 shows the coupling selected to connect the motor to the blade, an INTERFLEX coupling No. GE19 being selected.

Table 8 . Coupling selection

INTERFLEX No.	Torque nominal (Tn) in-lbs	Torque de diseño (Td) in-lbs	Hueco máximo con manzana: Estandar	Hueco máximo con manzana: Extra-Grande	RPM Máximas permisibles	Dimensiones en mm		
						A	B	L
GE 14	66	133	16		19,000	30	30	34
GE 19	89	177	19	24	14,000	40	40	64
GE 24	310	620	24	32	10,600	55	55	77
GE 28	841	1,682	28	38	8,500	65	65	88
GE 38	1,682	3,363	38	45	7,100	80	66	111
GE 42	2,345	4,691	42	55	6,000	95	75	125
GE 48	2,744	5,487	48	60	5,600	105	85	138
GE 55	3,319	6,638	55	70	4,750	120	98	156
GE 65	3,761	7,523	65	75	4,250	135	115	181
GE 75	8,629	17,257	75	90	3,550	160	135	206
GE 90	21,240	42,480	90	100	2,800	200	160	242

Source: [14]

Bearing selection

For a dynamic load of 52.26 Newton and 3600 rpm a deep groove ball bearing as shown in **Fig. 19** will be used.

- Shaft diameter=20mm
- Outside diameter= 47 mm
- Dynamic load= 52.26 newton

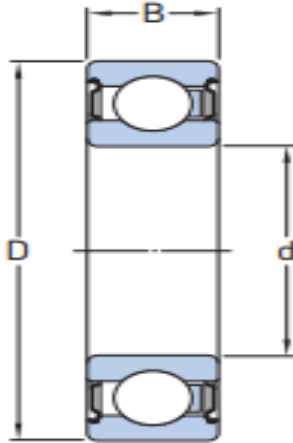


Fig. 19. Capped deep groove ball bearing E2. Source: [15]

A deep groove ball bearing **E2.6204-2Z** is selected according to **Table 9** for bearings with these characteristics.

Table 9 . SKF E2 deep groove ball bearings with plugs

Rodamientos rígidos de bolas SKF E2 tapados									
d 17 - 80 mm									
Dimensiones principales	Capacidad de carga básica		Carga límite de fatiga P_u	Velocidades nominales		Masa			
	d	D		B	C		C_0		
mm	kN		kN	r. p. m.	límite	kg			
17	35	10	5,85	3	0,127	49 000	25 000	0,039	E2.6003-ZZ
	35	10	5,85	3	0,127	-	15 000	0,038	E2.6003-2RSH
	40	12	9,56	4,75	0,2	41 000	21 000	0,065	E2.6203-ZZ
	40	12	9,56	4,75	0,2	-	13 000	0,065	E2.6203-2RSH
	47	14	13,8	6,55	0,275	37 000	19 000	0,12	E2.6303-ZZ
	47	14	13,8	6,55	0,275	-	12 000	0,112	E2.6303-2RSH
20	42	12	9,36	5	0,212	41 000	21 000	0,069	E2.6004-ZZ
	42	12	9,36	5	0,212	-	12 000	0,067	E2.6004-2RSH
	47	14	12,7	6,55	0,28	35 000	19 000	0,11	E2.6204-ZZ
	47	14	12,7	6,55	0,28	-	16 000	0,11	E2.6204-2RSH
	52	15	16,3	7,8	0,34	34 000	18 000	0,15	E2.6304-ZZ
	52	15	16,3	7,8	0,34	-	11 000	0,143	E2.6304-2RSH
25	47	12	11,1	6,1	0,26	35 000	18 000	0,08	E2.6005-ZZ
	47	12	11,1	6,1	0,26	-	11 000	0,077	E2.6005-2RSH
	52	15	13,8	7,65	0,325	30 000	16 000	0,13	E2.6205-ZZ
	52	15	13,8	7,65	0,325	-	10 000	0,13	E2.6205-2RSH
	62	17	22,9	11,6	0,49	-	28 000	0,23	E2.6305-ZZ
30	35	13	12,7	7,35	0,31	30 000	15 000	0,12	E2.6006-ZZ
	62	16	19,5	11,2	0,475	26 000	14 000	0,20	E2.6206-ZZ
	72	19	28,1	15,6	0,67	22 000	12 000	0,36	E2.6306-ZZ
35	62	14	15,3	9,15	0,39	26 000	13 000	0,15	E2.6007-ZZ
	72	17	25,5	15,3	0,64	22 000	12 000	0,30	E2.6207-ZZ
	72	17	25,5	15,3	0,64	-	7 300	0,28	E2.6207-2RST
	80	21	33,8	19	0,83	20 000	11 000	0,48	E2.6307-ZZ
40	68	15	15,9	9,65	0,405	24 000	12 000	0,19	E2.6008-ZZ
	80	18	30,7	18,6	0,78	20 000	11 000	0,38	E2.6208-ZZ
	80	18	30,7	18,6	0,78	-	6 500	0,35	E2.6208-2RST
	90	23	41	24	1,02	18 000	10 000	0,65	E2.6308-ZZ

Source: [15]

Mechanical seal selection

A stainless steel conical spring mechanical seal as shown in **Fig. 20** will be used.



Fig. 20 . Mechanical seal with conical spring. Source: [16]

Among its features and specifications are:

- Less possibility of blockage by solids
- Reduced sensitivity to axial deflection
- Longer life in corrosive environments

Using the data in **Table 10** and **Figure 21** as a guide, the second seal in the list with a diameter of 16 mm is selected.

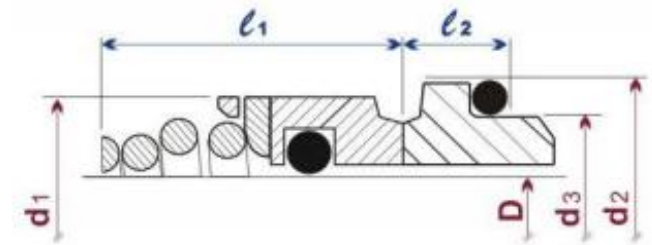


Figure 21 . Mechanical seal with solid stainless steel rotary. Source: [16]

Table 10 . Dimensions of mechanical seals

Dimensiones en mm.					
DIAM.	ROTATIVO		ESTACIONARIO		
D	d1	l1	d2	d3	l2
15	24	22	26.9	21	7
16	26	23	26.9	21	7
18	32 / 29	24	30.9	25	8
19	32 / 31	25	30.9	25	8
20	34 / 31	25	30.9	25	8
22	36 / 33	25	35.4	30	8
24	38 / 35	27	35.4	30	8
25	39 / 36	27	38.2	33	8.5
28	42 / 40	29	43.3	38	9
30	44 / 43	30	43.3	38	9
32	46	30	43.3	38	9
35	49	39	53.5	45	11.5
38	54 / 53	39	60.5	52	11.5
40	56	39	60.5	52	11.5
42	59 / 57	39	60.5	52	11.5
43	59	41	60.5	57	11.5
45	61	41	65.5	57	11.5
48	64	41	65.5	57	11.5
50	66	45	72.5	64	11.5
55	71	47	72.5	64	11.5
60	80 / 78	49	79.3	72	11.5

Source: [16]

Figure 23 shows the seal selected and installed in the mixing system.



Figure 22 . Installed mechanical seal

3. RESULT

Figure 23 and Figure 24 show the final construction of the industrial blender in frontal and isometric views.



Figure 23 . View 1, blender.



Figure 24 . View 2, blender.

After the blender was built and put into operation, it became evident that its maximum capacity is 60 liters. When a test was carried out with 50 liters of liquid milk, sugars and fats, the results were satisfactory due to the homogeneity and creaminess obtained.

The good result obtained is attributed to the capacity of the motor and to the geometry of the vessel, which was built with two angles to generate certain conicity; in the lower part the 45° angle has the function of forcing the mixture to descend to the bottom and go up through the blades, guaranteeing its complete liquefaction. The vertices of the upper part of the vessel, since the bending radius is small, make it behave as a deflector, causing the mixture passing through the blades to reach these vertices, collide with one part and return to the center of the vessel, generating great turbulence in the mixing, and the remaining part descends again towards the blades.

To put in context, considering that the capacity of the industrial blender vessels commonly used in these processes is around 15 liters of mixture and that the blending is done for 4 minutes, the time it takes to prepare 300 liters of mixture is around one hour and 20 minutes, associated to this, it is necessary to blend 20 times to complete the 300 liters at a temperature of 35°C. This completes the first liquefying process.

Subsequently, when the mixture reaches 60°C, the process of liquefying the same 300 liters must be repeated, adding fats for another hour and 20 minutes; this would be the second liquefaction. The final liquefaction is carried out when the mixture is at 85°C, from here the mixture passes to the agitation tanks.

On average, the preparation of the mixture takes four hours, during which time an extra effort must be made to transfer the mixture to the funnel where it is circulated to reach the pasteurizer, to this time must be added the time spent by the operators in transferring the mixture each time it is liquefied to the funnel to circulate it, making it reach the pasteurizer.

Taking into account these data and comparing the blending capacity of the previous blender with the new blender, it is evident that the blending volume increases by 50 liters during an average time of 8 minutes, i.e., 6 blends are needed to mix the same 300 liters during 48 minutes. The three blending processes would take only 2 hours and 24 minutes where the operators will not be in contact with the raw material, they will only have the task of turning on the blender and the centrifugal pump to circulate the mixture when it is ready.

4. CONCLUSION

With the liquefying system developed, the mixing process can be carried out between 15 and 50 liters of ice cream mix, reducing the mixing time to 2 hours, when previously the time was approximately five hours. In terms of hygiene, there was a reduction of direct contact between product-operator of about 50%. On the other hand, the operators are no longer exposed to the direct steam coming out of the hot mix.

With the new system, the blending preparation time was reduced by two hours and 36 minutes, which indicates that the blender built meets all the requirements to guarantee the quality and correct preparation of the mixture and, above all, to protect the integrity of the operators.

Acknowledgement

The authors would like to express their gratitude to the food laboratory staff at the University of Pamplona's master's room facilities.

REFERENCES

- [1] A. Almena, P. J. Fryer, S. Bakalis, and E. Lopez-Quiroga, "Local and decentralised scenarios for ice-cream manufacture: A model-based assessment at different production scales," *J. Food Eng.*, vol. 286, p. 110099, Dec. 2020, doi: 10.1016/j.jfoodeng.2020.110099.
- [2] K. Cronin and D. Ring, "Plant, Equipment and Utilities: Mixers and Agitators," in *Reference Module in Food Science*, Elsevier, 2020. doi: 10.1016/B978-0-12-818766-1.00123-9.
- [3] H. M. Rodriguez Magaña, «Análisis HACCP del proceso de elaboración de azúcar y estandarización de la ecología microbiana presente en campo y fabrica en el ingenio quesería del grupo BSM», Instituto Tecnológico de Colima, Technical Report, 2018. Accedido: ago. 14, 2021. [En línea]. Disponible en: <https://dspace.itcolima.edu.mx/xmlui/handle/123456789/1440>
- [4] J. M. Calle Calle, «Diseño y fabricación de un fluidificador semindustrial», 2002, Accedido: ago. 14, 2021. [En línea]. Disponible en: <http://dspace.uazuay.edu.ec/handle/datos/2648>
- [5] M. Angel y Q. Solano, «Operaciones Unitarias II. Agitación y Mezclado Universidad Nacional Del Centro de Perú.», p. 15, 2013.
- [6] M. D. Sinnott, S. M. Harrison, and P. W. Cleary, "A particle-based modelling approach to food processing operations," *Food Bioprod. Process.*, vol. 127, pp. 14-57, May 2021, doi: 10.1016/j.fbp.2021.02.006.
- [7] E. Bohorquez Ariza, "Universidad Nacional Abierta y a Distancia Escuela De Ciencias Básicas, Tecnología e Ingeniería Programa De Ingeniería De Alimentos". <https://docplayer.es/5726264-Universidad-nacional-abierta-y-a-distancia-escuela-de-ciencias-basicas-tecnologia-e-ingenieria-programa-de-ingenieria-de-alimentos.html> (accessed Aug. 14, 2021).
- [8] R. W. Caiza Martillo, «Diseño, construcción y operación de un mezclador para producir abono orgánico a partir de los residuos orgánicos», jun. 2013, Accedido: ago. 14, 2021. [En línea]. Disponible en: <http://dspace.ups.edu.ec/handle/123456789/5312>
- [9] R. Avila-Chaurand, L. Prado-León, y E. González-Muñoz, *Dimensiones antropométricas de la población latinoamericana : México, Cuba, Colombia, Chile / R. Avila Chaurand, L.R. Prado León, E.L. González Muñoz.* 2007.
- [10] "XVIGAS beam analysis download | SourceForge.net." <https://sourceforge.net/projects/xvigas/> (accessed Aug. 14, 2021).
- [11] "BROOKFIELD DVE. Digital Viscometer. Manual No. M15-356-B0916." [Online]. Available at: <https://www.brookfieldengineering.com/>
- [12] A. F. Méndez-Sánchez, L. Pérez-Trejo, y A. M. P. Mercado, «Determinación de la viscosidad de fluidos newtonianos y no newtonianos (una revisión del viscosímetro de Couette)», vol. 4, n.º 1, p. 9, 2010.
- [13] C. Delgado, «Diseño de elementos de máquinas.pdf», Accedido: ago. 14, 2021. [En línea]. Disponible en: https://www.academia.edu/38450613/Dise%C3%B1o_de_elementos_de_m%C3%A1quinas_pdf
- [14] "acoples_interflex.pdf". Accessed: Aug. 14, 2021. [Online]. Available at: https://www.intermec.com.co/pdf/acoples_interflex.pdf
- [15] "Deep groove ball bearings | SKF | SKF." <https://www.skf.com/co/products/rolling-bearings/ball-bearings/deep-groove-ball-bearings> (accessed Aug. 14, 2021).
- [16] "Machined seals | SKF." <https://www.skf.com/co/products/industrial-seals/machined-seals> (accessed Aug. 14, 2021).